

Calculation of Key Characteristics for Ion Ensembles in Quadrupole Ion Traps Without Utilizing Trajectory Simulations

D.E. Goeringer¹, L.A. Viehland², and D.M. Danailov²

¹Oak Ridge National Laboratory, Oak Ridge, TN 37831-6131; ²Chatham College, Pittsburgh, PA 15232-2813



OVERVIEW

Goal:

- To improve the conceptual understanding of physicochemical processes in RF ion traps by using mathematical/computational methods to develop a comprehensive model, and to apply the knowledge gained to enhance their capabilities for fundamental and analytical chemical investigations

Methods:

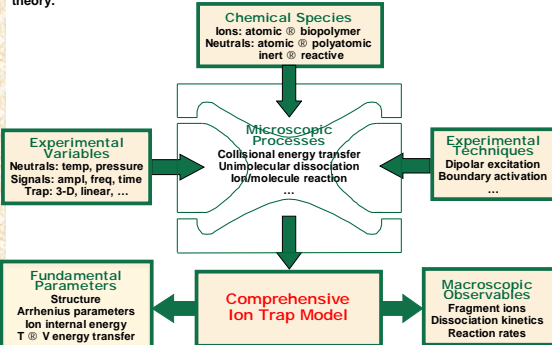
- Starting from the Boltzmann equation, moment methods were used to develop a two-temperature model theory for ion motion in devices where the electric field is time- and position-dependent
- Using analytical expressions for the trapping and supplemental electric fields, differential equations representing the first-order (momentum-transfer) approximation of the theory were written for ideal and non-ideal ion traps
- Mathcad code was developed to solve the differential equations and perform the necessary calculations to obtain various quantities of interest

Results:

- The set of coupled differential equations presented here, which do not appear to have been given previously, directly provide average velocity and temperature (energy) information for an ion ensemble as a function of time and of position in the apparatus without trajectory simulations. This is because the Boltzmann equation, from which the coupled equations were developed, reflects changes to the ion distribution as a whole.
- New dimensionless parameters for the ring electrode voltages take into account nonlinearities and differences in trap configurations. Their use in calculations at the design stage for new ion trap configurations might reduce potential chemical mass shifts. Similarly, new dimensionless parameters for the voltages applied to the endcaps should allow easier comparison between ion trap configurations during experiments involving such voltages.
- Calculation results suggest that ion heating in the resonance excitation process is primarily due to increased power absorption from the RF field rather than from the dipolar excitation signal as previously thought. The dipolar excitation signal mainly serves to move ions into regions of the ion trap where the RF electric field, and thus ion RF heating, is greater than near the trap center.

INTRODUCTION

Development of a comprehensive model for the physicochemical processes in RF ion trap mass spectrometers is a non-trivial undertaking. The fast RF ion motion modulates lower frequency secular oscillations. Because typical operation involves the use of buffer gas at 0.1-1 Torr, ion-neutral collisions also can change the phase of these oscillations, resulting in RF energy gain or loss and a change in amplitude. Additionally, energy transfer and reactions that occur between colliding ion-neutral pairs are crucial to the analytical applications of the devices. Furthermore, knowledge of ion temperatures (energies) and distributions is key to fundamental studies. Thus, formulation of a comprehensive model requires integration of theoretical aspects for time- and position-dependent, nonlinear electric fields, ion transport in gases, collisional energy transfer, ion-molecule reactions, and unimolecular dissociation theory.



Due to the complex nature of the ion trap operating environment described above, simple phenomenological equations are inadequate for treating ion processes accurately and completely in the devices. Thus, our comprehensive model is developed around the Boltzmann equation, which describes the effects of applied electric fields and collisions on the ion distribution function, $f(r,v,t)$. Because the Boltzmann equation reflects changes to the ion distribution as a whole, subsequent transformation into moment equations enables the ensemble average value for any property that is a function of the ion velocity to be determined as a function of time and position from the corresponding moment. The moment equations also are subject to limitations of the Boltzmann equation from which they are derived; the significance to this work is that applicable systems are comprised of trace concentrations of atomic ions moving through a dilute buffer gas of unreactive atomic neutrals.

THEORY

Knowledge of the ion distribution function would enable any moment, $J_i(r,t)$, (or related quantity) to be found via integration, viz.:

$$\bar{J}_i(r,t) = \frac{\int J_i(v)f(r,v,t)dv}{\int f(r,v,t)dv}$$

However, solving the Boltzmann equation directly for $f(r,v,t)$ is generally not possible. An alternative method for determining moments involves transforming the Boltzmann equation into a differential equation that describes the desired moments themselves, thus making it possible to find the corresponding properties without determining $f(r,v,t)$ directly.

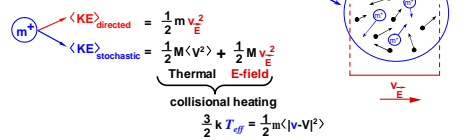
The general moment equation is formed by multiplying the Boltzmann equation by a general function, $J_i(v)$, of the ion velocity, and then integrating over all velocities. The first (momentum-transfer) approximation of the moment equation is obtained by assuming that terms involving $(\nabla \cdot \nabla)$ and $(\nabla \cdot \nabla - \nabla \cdot \nabla)$, which appear in the transformed equation, are negligible. The action of the adjoint, \bar{J}_i , of the Boltzmann collision operator can be thought of as producing the average rate of change in J_i due to collisions.

$$\frac{d}{dt} \bar{J}_i - \frac{q}{m} \mathbf{E} \cdot \nabla \bar{J}_i = \bar{J}_i$$

Rather than using relative kinetic energy in describing gaseous ion transport, it is often practical to consider a directly related quantity, the ion effective temperature (T_{eff}). In the context of mass spectrometry, the effective temperature has often been viewed as the temperature characterizing a Maxwell-Boltzmann energy distribution of ions that would produce a specified rate for a well-characterized, temperature-dependent ion process. In contrast, the effective temperature in this work describes the state of the system as related to the relative ion-neutral kinetic energy.

Overall trapped ion motion is superposition of:

- Large-scale motion (secular and micromotion) within the ion trap is due to the position- and time-dependent trapping electric field
- Spatial gradients of the ion number density are much smaller than spatial variations of the electric field, so the electric field within the ion cloud is position-independent and small-scale motion is accurately described by the Boltzmann equation



$$T_{eff} \text{ @ } \text{ion-neutral COM kinetic energy available for conversion to internal energy}$$

The energy moment for T_{eff} is $J(v) = \frac{1}{2} m v^2$, and the corresponding moment equation is:

$$\frac{d}{dt} T_{eff} - \frac{2q}{3k} \frac{M}{m+M} \mathbf{E} \cdot \nabla + \frac{2m\mathbf{x}(T_{eff})}{m+M} [T_{eff} - T] = 0$$

Solution of the moment equation above for the effective temperature requires another moment equation describing variations in v , which can be obtained using $J(v) = v$.

$$\frac{d}{dt} \bar{v} - \frac{q}{m} \mathbf{E} + \mathbf{x}(T_{eff}) \nabla = 0$$

The system of differential equations, coupled through the collision frequency for momentum transfer, x , can be solved for the four quantities, \bar{v}_x , \bar{v}_y , \bar{v}_z and T_{eff} , each as a function of position and time. Note that the components of the average ion velocity may not be equated to the time derivative of the position dz/dt for a single ion.

$$m \equiv \text{ion mass} \quad M \equiv \text{neutral mass} \quad m \equiv \text{ion-neutral reduced mass} = \frac{mM}{m+M}$$

$$q \equiv \text{ion charge} \quad T \equiv \text{neutral temperature} \quad N \equiv \text{neutral number density}$$

$$U_R \equiv \text{amplitude of DC potential on ring electrode}$$

$$V_R \equiv \text{amplitude of ring electrode AC potential, with angular frequency } \Omega$$

$$U_D \equiv \text{amplitude of DC potential on endcap electrodes}$$

$$V_D \equiv \text{amplitude of endcap electrode AC potential, with angular frequency } \omega$$

$$r_0 \equiv \text{radius of ring electrode} \quad 2z_0 \equiv \text{shortest distance between endcaps}$$

Dependence of Ion Secular Frequencies On Trap Configuration and Spatial Location Can Be Calculated a priori

In an ideal trap the secular ion frequencies, f_{i0}^{ideal} , are position-independent.

$$f_{i0}^{ideal} = \frac{b_i(a_i, q_i)}{2} \frac{\Omega}{2\pi} \quad u = x, y, z$$

The coefficient $b_i(a_i, q_i)$ is given by a continued fraction expansion in terms of the standard parameterized variables for the ion trap.

$$a_i = -2a_i = \frac{-16eU_R}{m(\tilde{a}_i^2 + 2z_0^2)\tilde{\Omega}^2} \quad u = x, y \quad q_i = -2q_i = \frac{8eV_D}{m(\tilde{a}_i^2 + 2z_0^2)\tilde{\Omega}^2}$$

However, for a non-ideal trap, f_{i0} varies with the amplitude of ion oscillation due to the nonlinear electric fields. This variation can be calculated a priori if the parameterized variables are written in a modified form, \tilde{a}_i and \tilde{q}_i , based on a multipole expansion, F , for the total electric potential in the trap:

$$\Phi(x, y, z) = F_R \sum_{n=0}^{\infty} A_n^R \left(\frac{r}{r_0}\right)^{2n} P_{2n}^0\left(\frac{z}{z_0}\right) + F_D \sum_{n=0}^{\infty} A_n^D \left(\frac{r}{r_0}\right)^{2n+1} P_{2n+1}^0\left(\frac{z}{z_0}\right)$$

F_R and F_D are the ring and endcap potentials, respectively. The dimensionless expansion coefficients, A_n , for the Legendre polynomials, P_n , are dependent on the specific physical configuration. The modified parameterized variables are then:

$$\tilde{a}_i = \frac{\tilde{a}_i}{q_i} = \frac{-A_0^R (\tilde{a}_i^2 + 2z_0^2)}{2r_0^2} \left[1 + \frac{A_2^R}{A_0^R} \frac{12z_0^2 - 3(\tilde{a}_i^2 + y^2)}{2r_0^2} \right] \quad u = x, y$$

$$\tilde{q}_i = \frac{-A_0^D (\tilde{a}_i^2 + 2z_0^2)}{2r_0^2} \left[1 + \frac{A_2^D}{A_0^D} \frac{24z_0^2 - 180z_0^2(\tilde{a}_i^2 + y^2) + 15(\tilde{a}_i^2 + y^2)^2}{8r_0^6} \right]$$

The dimensionless parameters, \tilde{a}_i and \tilde{q}_i , now include terms for distance from the trap center and expansion coefficients to take into account nonlinear variations with position and differences in configuration. Thus, the position- and configuration-dependent secular frequencies can be calculated from the same continued fractions expression as before, but with \tilde{a}_i and \tilde{q}_i substituted for a_i and q_i .

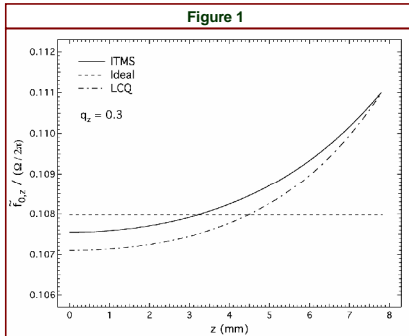


Figure 1 shows values of \hat{f}_{i0} (normalized by $\Omega/2\pi$) at $q_i = 0.3$, calculated as a function of axial distance from the trap center for the ITMS, ideal, and LCQ configurations. Because a_i and q_i do not vary with axial position in the ideal trap, is invariant over the indicated z range. Over the same axial distance, the relative variation in the normalized value of \hat{f}_{i0} is slightly larger for the LCQ than for the ITMS. Such calculations might potentially be used at the design stage for new ion trap configurations to reduce potential chemical mass shifts.

We note that it is also possible to parameterize the voltages applied to the endcaps, as proposed below using b (DC voltages) and d (AC voltages), in a manner similar to that done with the ring electrode. This would allow easier comparison between ion trap configurations during experiments involving such voltages. We have also developed equations for modified versions of the endcap parameters, \tilde{b} and \tilde{d} , using the expansion coefficients above.

$$\tilde{b}_i = -2\tilde{b}_i = \frac{-16eU_D}{m(\tilde{a}_i^2 + 2z_0^2)\tilde{\Omega}^2} \quad u = x, y \quad \tilde{d}_i = -2\tilde{d}_i = \frac{8eV_D}{m(\tilde{a}_i^2 + 2z_0^2)\tilde{\Omega}^2}$$

RESULTS AND DISCUSSION

Calculations Indicate That the Stability Region is a Function of the Dipolar Signal Amplitude During Resonance Excitation

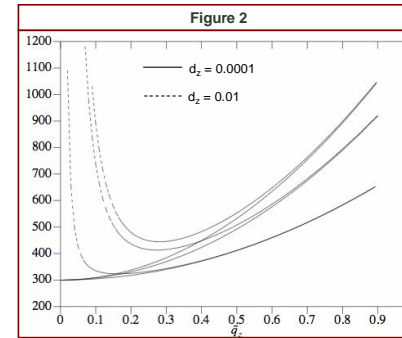
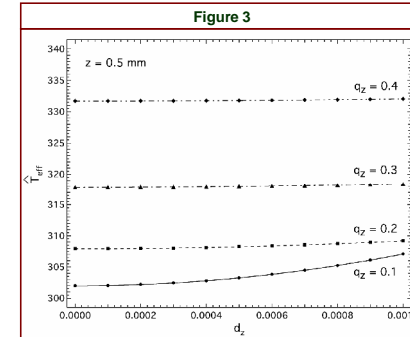
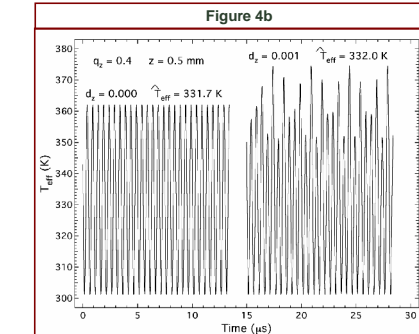
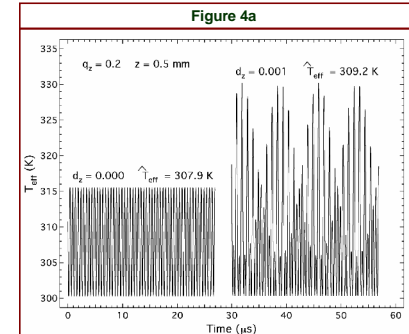


Figure 2 indicates the dependence of the effective temperature upon q_i when $d_i > 0$ and the trap is at resonance, i.e. the frequency of the dipolar excitation signal applied to the endcaps is equal to the secular frequency of ion oscillation. The plotted T_{eff} curves represent the time average of the effective temperature over ten cycles of the dipolar signal applied to the endcaps with $d_i = 0.0001$ (102.3 mV_{p-p}, solid lines) and 0.01 (10.23 V_{p-p}, dotted lines). In decreasing order, the solid and dashed pairs correspond to the ITMS, ideal, and LCQ traps, respectively. In addition, $m/z = 100$, the He pressure is 1 mTorr, $x = y = 0$ and $z = 1$ mm. For q_i values above 0.27, the average effective temperature increases with q_i for both values of d_i . However, the $d_i = 0.0001$ values decrease toward 300 K as q_i decreases towards zero, while for $d_i = 0.01$ the average effective temperatures reach a minimum and then begin to rapidly increase again with further decreases in q_i . This is attributed to the fact that the region of stability has a lower limit of $q_i = 0$ when $a_i = b_i = d_i = 0$, but as d_i increases the q_i value characterizing the lower limit of the stability region increases as well (i.e., ion ejection occurs).

Calculations Indicate That Increases in T_eff During Resonance Excitation Are Primarily the Result of Power Absorption from the RF Trapping Field



Figures 3 and 4a, b are revealing in regard to the underlying means by which the increases in T_{eff} occur. Figure 3 shows T_{eff} curves at 0.5 mm calculated for situations in which a dipolar excitation signal is applied to the endcaps of an ideal trap (in addition to application of the main trapping voltage to the ring). For each q_i value, the frequency of the applied signal corresponds to the axial secular frequency, that is, the dipolar signal is resonant with the ion secular oscillations. The plotted T_{eff} values represent the time average of T_{eff} over ten cycles of the appropriate excitation frequency. Each of the four curves covers a d_i range from 0.000-0.001, which represents a peak-peak amplitude range of 0-1023 mV. Note, however, that when $d_i = 0.000$ the situation corresponds to an ion trapping scenario, so any increase in T_{eff} above thermal is due to ion RF heating only. Over the indicated d_i range in Figure 3, the T_{eff} increase due to dipolar excitation is small for any individual curve (e.g., only 1.3 K and 0.3 K for $d_i = 0.001$ at $q_i = 0.2$ and 0.4, respectively). In contrast, additional RF heating due to changes in q_i (μV_e) results in significantly larger T_{eff} increases (e.g., 7.9 K and 31.7 K for $d_i = 0.001$ at $q_i = 0.2$ and 0.4, respectively). These effects also can be seen in the time-dependent T_{eff} plots in Figures 4a and 4b below.



4a and 4b show segments of the calculated time-dependent T_{eff} data from which the T_{eff} data points at $[q_i = 0.2, 0.4; d_i = 0.000, 0.001]$ in Figure 3 were derived. When $d_i = 0.000$ the time-dependent T_{eff} values vary at twice the main RF frequency, since power is absorbed during both positive and negative phases of the main RF. Application of the dipolar excitation signal at $d_i = 0.001$ results in the T_{eff} oscillations being modulated at twice the dipolar excitation frequency. Although the depth of modulation is greater for $q_i = 0.2$ than for $q_i = 0.4$ (because $V_R(q_i = 0.2) < V_R(q_i = 0.4)$), in each case it is considerably less than the amplitude of oscillations at twice the RF frequency. These results suggest that ion heating in the resonance excitation process is primarily due to increased power absorption from the RF field rather than from the dipolar excitation signal. The dipolar excitation signal mainly serves to move ions into regions of the ion trap where the RF electric field, and thus ion RF heating, is greater than near the trap center.

SUMMARY

- The differential equations presented here, which do not appear to have been given previously, tend to complement those presented in previous ion trap studies. This is because of the difference in viewpoint between the present approach, which focuses on average behavior of an ion ensemble, and others that concentrate on the individual trajectories of single (or multiple) ions.

- The moment equations developed here can be solved directly (ordinarily, by numerical means) for the average ion velocity and effective temperature as a function of position and time. However, they can not reveal any positional or temporal information for a single ion (as is produced in the standard output from the widely used ion trap simulation program ITSIM). Conversely, many individual ion trajectories must be simulated and the resulting data collected and post-processed outside that program to yield similar ensemble average and number density information.

- The moment equations incorporate modified forms of commonly used parameterized variables for the DC and AC ring voltages, and new forms that account for the voltages applied to the endcaps. Besides extending the applicability of the moment equations to non-ideal quadrupole ion traps, the modified versions of the parameterized variables can have additional utility. Calculation of the spatial dependence of ion secular oscillation frequencies is demonstrated as an example.

- Calculations suggest that increases in ion effective temperature during resonance excitation are due primarily to power absorption from the main RF trapping field rather than from the dipolar excitation signal. The dipolar excitation signal apparently serves mainly to move ions into regions of the ion trap where the RF electric field, and thus ion RF heating, is greater than near the trap center.

- In future papers we expect to extend this work to include molecular ions and linear traps, but the equations developed here are applicable to other RF multipole devices as well. We also intend to consider space charge effects by including Poisson's equation.

REFERENCES

- G.H. Wannier *Bell System Tech. J.* **32**, 170 (1953).
- L.A. Viehland, E.A. Mason *Ann. Phys. (N.Y.)* **81**, 499 (1975).
- E.A. Mason, E.W. McDaniel *Transport Properties of Ions in Gases* (Wiley, New York, 1988).
- R.K. Julian, H.-P. Reiser, R.G. Cooks *Int. J. Mass Spectrom. Ion Processes* **123**, 85 (1993).
- D.E. Goeringer, S.A. McLuckey *J. Chem. Phys.* **104**, 2214 (1996).
- R.E. Robson, R.D. White, T. Makabe *Ann. Phys. (N.Y.)* **261**, 74 (1997).
- L.A. Viehland, D.E. Goeringer *J. Chem. Phys.* **120**, 9090 (2004).
- D.E. Goeringer, L.A. Viehland *J. Phys. B* **38**, 4027 (2005).

ACKNOWLEDGMENTS

Research at ORNL sponsored by the Division of Chemical Sciences, Geosciences, and Biosciences, Office of Basic Energy Sciences, U.S. Department of Energy, under contract No. DE-AC05-00OR22725 with Oak Ridge National Laboratory, managed and operated by UT-Battelle, LLC. Research at Chatham College was supported by the National Science Foundation under grant CHE-0092436.